

The New HEMS Modelling of Human Heart

Fikret Yalcinkaya and Ertem Kizilkaplan

Abstract— The new version of the hydro-electro-mechanical system (HEMS) is modeled via 14 serially connected electrical equivalent circuits resulting in an integrated equivalent circuit. The new model accepts a group of variables and even examines the interaction between them. This paper introduces an improved integrated new model of the heart by replacing the monolithic equivalent structures with segmental comprehensive equivalents. Windkessel Model (WM) is a model of the relationships between aorta, aortic valve and left ventricle. Based on WM, the integrated new model was developed and simulated. The model's main focus is to define the dynamic properties of the system by a set of ordinary differential equations, and solving them using Ode23, a method for the solution of a closed-loop system. Using Matlab based Ode23 method; time-dependency of pressure, volume and flow were obtained. In case, short computation time and high accuracy are needed, then Ode23 is used. The model may be used to analyze complex processes in the heart and blood vessels. The new HEMS model has potential use for hemodynamic simulation of diseases, cardiovascular disorders, and special congenital heart diseases; such as ASD, VSD and PDA.

Index Terms— Time-dependent average pressure, biomedical engineering, medical control systems, medical simulation.

I. INTRODUCTION

TO OVERCOME critical and challenging heart conditions and to understand the functionality of the cardiovascular system (CVS), various models of human heart have been studied using physical models of the real and the artificial systems, based on the reference test domain [1]. The model of Windkessel is a famous example of such a discrete model [2,3]. Due to the complex nature of the human heart, models claiming to be sufficient standalone propose that the basic components and functions of the heart should separately be considered. Although computer analysis of numerical models has replaced physical models in many cases, electrical equivalent circuits and numerical analysis methods are now widely being used in

FIKRET YALCINKAYA, is with Department of Electrical and Electronics Engineering, Kirikkale University, Kirikkale, Turkey, (e-mail: fyalcinkaya@kku.edu.tr).

 <https://orcid.org/0000-0002-2174-918X>

ERTEM KIZILKAPLAN, is with Department of Electrical and Electronics Engineering, Kirikkale University, Kirikkale, Turkey, (e-mail: ertem.kizilkaplan@gmail.com).

 <https://orcid.org/0000-0003-2602-4804>

Manuscript received Jan 22, 2022; accepted July 22, 2022.

DOI: [10.17694/bajece.1061718](https://doi.org/10.17694/bajece.1061718)

addition to mathematical models in testing the control and stability of the cardiovascular system for the sole benefit of the heart and its functions [4]. Because the human cardiovascular system is an extremely nonlinear integrated structure in which electrical, mechanical and hydraulic components all work together in harmony. In this context, 0, 1, 2 or 3 dimensional models have been used in order to provide a better understanding of functionality and the simulation of blood flow in the human cardiovascular system and different calculation techniques have been developed using experimental methods [5]. Although these approaches simulate only certain sections of the cardiovascular system, they often reveal that the systems are quite difficult and unstable, and nearly unsolvable nonlinearity problems arise.

The difficulty of cardiovascular system modelling arises from its multifunctionality and compartmentalized nonlinear structure. In order to overcome this issue, due to the difficulties encountered in integrating modelling of the whole system, instead of modelling all the subsystems of the real system, it is preferred to model some parts of it independently [6], in order to reduce the problem complexity, and developing cardiovascular system new models can produce healthy hemodynamic data that mimic diseases to certain extent [7]. The hemodynamic measurements of a healthy person with a modified Windkessel model were used to analyze the hemodynamic data of congenital heart diseases, such as hypoplastic left heart syndrome (HLHS) [8].

Cardiovascular system modelling requires not only electrical simulation, the integrated electro-mechanical response of the heart, but also its two-dimensionality- hydraulic and pneumatic –as well, as that increases the complexity of the heart system; its complexity increases due to the hydraulic structure of the heart and the pneumatic pressure of the lung on the heart cycle. Modelling attempts integrating or cascading pneumatic effect to the hydro-electro-mechanical effect are a few in the literature. For this purpose, a new version of cardiovascular system model was attempted in this paper, and attention was paid to include more details than the HEMS model and to use quite a lot parameters [9].

The new HEMS model can evaluate and verify the effects of a group of variables at the same time and even make it possible to examine the interaction between more than one variable. Autocad based anatomical 3D drawings of all subsystems of the heart have been produced in order to get the best results specific to modelling and physiological requirements. 3D drawings and models are used to facilitate intermediate version development to achieve the integrated HEMS model. Because, in order to

integrate nonlinear complex biological structures and independent models, the structures described as interface and their models are needed [10].

In order to examine the hemodynamic of the cardiovascular system (CVS), first of all, the hydro-electro-mechanical system of the heart was modelled through 14 serially connected electrical equivalent circuits which demonstrates the integrated form of all subsystems developed. In the new HEMS model, a total of 28 equations (Eq. 4 – Eq. 31) were developed and used for the pressure and flow values at the outlets of all segments. In addition, pressure, volume and flow graphs for the whole circuit were obtained using the Matlab Ode23 method.

II. METHOD

The cardiovascular system requires the integration of four basic structures; these vital structures are the heart and triple vascular network. This network system is a network of arteries, veins, and capillaries. Blood circulates in the cardiovascular system through this network with the effect of pressure produced by the heart. Blood is a non-Newtonian fluid that completes its cycle through and by these structures. Events and processes occurring during the cardiac cycle are shown in The Wigger's diagram [11].

It is necessary to simulate the flow waveforms to describe the two different phases of the cardiac cycle, the systole and diastole. Under normal conditions, 60 to 100 impulses per minute originate from the sinus node (SA node) to trigger the heartbeat. The heartbeat time (Heart Period-HP) used in our model is 0.83 seconds (corresponds to 72 beats / minute). During this period, the systole time was 0.33 s and the diastole time was 0.50 s.

The time cycle in the heart begins with the activation of the heart muscle around the right atrium near the upper vena cava. The heart muscle surrounding the atriums and ventricles undergoes contraction and relaxation during a cycle. This contraction and relaxation in the heart is associated with intracellular calcium (Ca^{+2}) ion movement.

The activation function has been obtained in atrium over a heart cycle using MATLAB. The general idea is to discretize the given function, evaluating the function at different times separated by the time interval dt . dt is the time interval between two consecutive samples and it has been selected to be 0.01 s. The total number of samples for which the function evaluated depends on the heart period and the number of heart cycles represented. For dt -equals 0.01 s and period HP-equals 0.83 s then the number of samples is determined. This time interval seems ideal for the representation of both the flow and the pressure as these variables vary along the heart cycle. The total number of samples for which the activation function generated in the atria and ventricles will be evaluated depending on the heart period and the cardiac cycle time shown. A graphical representation of the activation function is given below for the first cardiac cycle. (Fig. 1)

The walls in the ventricles are characterized by time-varying elastic functions that relate instantaneous pressure and volume. These flexibility functions provide a smooth transition from a nonlinear diastolic pressure-volume curve (EDV) to a linear

systolic pressure-volume relationship (ESV). In our model, in order to represent the contraction and relaxation changes in each cardiac chamber, a time dependent sinus wave activation function was created for the ventricle and atria. The right and left ventricles are modelled as variable capacitors to calculate the relationship of pressure, volume and time, as well as viscous losses due to their characteristic flexibility and activation function. The time-dependent end-diastolic elastance (its hardness) of the right and left ventricles is shown in E_d , equation 1 with its general expression [12].

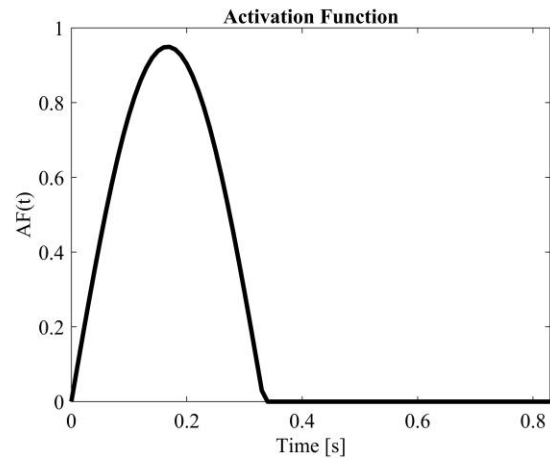


Fig. 1. Activation function for the first cardiac cycle

$$E_d(t) = AF(t) \cdot E_{DV} + [1 - AF(t)] \cdot E_F \quad (1)$$

According to this formula, $E_d(t)$ is determined as a time-varying parameter of flexibility according to the maximum and minimum values of the activation function. E_F refers to the harmonic factor created for the ventricles in this change, E_{DV} is the diastolic stiffness created for the right and left ventricles, and $AF(t)$ is the generated activation function.

The blood flow and its dynamics are used to study the hemodynamics of healthy and diseased blood vessels, vascular specific conditions, and the cardiovascular system. Hemodynamics can be defined as the physical principles that govern blood flow based on the fundamental laws of physics. Of these basic laws, Ohm's law can be expressed for the cardiovascular system as seen below. In addition, the relationship between the electrical, mechanical and hydraulic parameters is given as in TABLE I.

$$\Delta Q = \frac{\Delta P}{R} \quad (2)$$

TABLE I. ELECTRICAL, MECHANICAL AND HYDRAULIC PARAMETERS

	Symbol	Element	Unit
Electrical System	R	Resistance	ohm
	L	Inductance	s·ohm
	C	Capacitance	s/ohm
	U	Voltage	volt
	q	Charge	amper·s
	I	Current	amper

Mechanical System	B	Damping Rate	N·s/m
	M	Mass	kg
	K	Spring Rate	N/m
	F	Force	N
	x	Displacement	m
	v	Velocity	m/s
Hydraulic System	R	Blood Viscosity	mmHg·s/ml
	L	Blood Inertance	mmHg·s ² /ml
	C	Wall Compliance	ml/mmHg
	P	Pressure	mmHg
	V	Volume	ml
	Q	Blood Flow	ml/s

Windkessel modeling is used to represent the connection between hydraulic structure and electrical structure equivalent circuits. As the Windkessel model is the most accepted form of discrete modeling, it allows us to understand the relationship between blood pressure and blood flow in the aorta (Fig. 2 (a)- Fig. 2 (b)).

The similarity relationship between the electrical, mechanical and hydraulic parameters of the circuit elements to be created for modeling the cardiovascular system is shown in TABLE I, and with this analogy, parts of the system model can be combined with separate components to model the physical systems with interconnected components. According to this analogy; in case of electrical systems, these elements include resistors (R), capacitors (C), and inductors (L). For mechanical systems these include inertia (masses-M), springs (K) and shock absorbers (or friction elements-B). For hydraulic systems, these include flow resistance/viscosity (R), inertness (L), and chamber compliance (reservoir capacity) (C). Each segment of the circulatory cycle is modeled through a series of equations, describing the relationships, that give the correlations between the parameters of pressure (P, mmHg), volume (V, ml), and flow (Q, ml/s) associated with that specific segment. However, the desired average pressure and volume distribution determine the parameter values of compliances and resistances. For example, the time-dependent pressure and flow equations at the nodes that govern the aortic hydraulic components are obtained as follows:

$$\Delta P = L \frac{dQ}{dt} = \frac{\Delta V}{C} \tag{3}$$

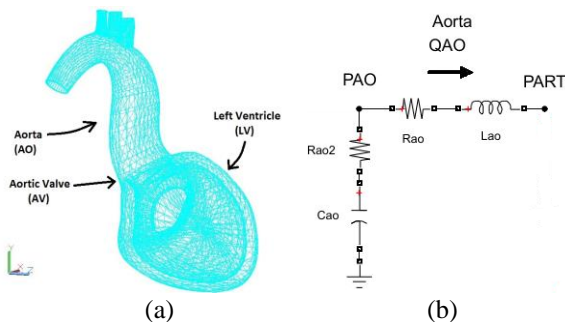


Fig. 2 (a) Autocad 3d representation of Aorta-Left Ventricle. (b) Hydraulic circuit of the Windkessel effect (model) between the aorta - left ventricle.

In equations (4) and (5), time dependent average pressure (P_{AO}) and flow (Q_{AO}) equations are obtained for the aortic part of the heart:

$$P_{AO}(t) = \frac{V_{AOI}(t) - V_{AOU}(t)}{C_{ao}} + R_{ao2} \cdot [Q_{LVI}(t) - Q_{AOI}(t)] \tag{4}$$

$$\frac{dQ_{AO}(t)}{dt} = \frac{P_{AO}(t) - P_{ART}(t) - [R_{ao} \cdot Q_{AOI}(t)]}{L_{ao}} \tag{5}$$

In equations (6) and (7), time-dependent average pressure (P_{ART}) and flow (Q_{ART}) equations are obtained for the heart arteries, where P_{CAPS} is time-dependent average pressure for the heart capillaries.

$$P_{ART}(t) = \frac{V_{ARTI}(t) - V_{ARTU}(t)}{C_{art}} \tag{6}$$

$$Q_{ART}(t) = \frac{P_{ART}(t) - P_{CAPS}(t)}{R_{art}} \tag{7}$$

The components of 3-D functional anatomy in which all the parts of the new version of hydro-electro-mechanical system developed are independently modeled and are given below. Representation sequencing of blood flow in the heart segments is drawn in 3-D forms by using Autocad of four compartments and other subsystems components, shown in Fig. 3.

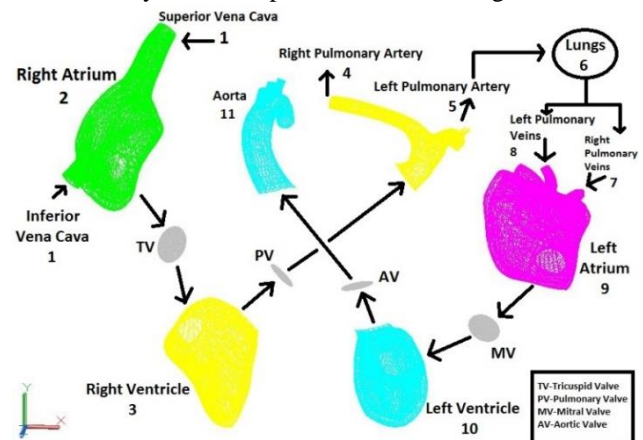


Fig. 3. Representation of blood flow in heart sub-segments drawn in 3D with Autocad

The analytically solvable hydraulic, electrical and mechanical models are designed to study the entire subsystem of specific organs (eg, the heart). Because of the multi-systems character of the human body total system and the multi-subsystems of each system make biological modeling extremely complex, as there are numerous variables that affect the functions, properties, and response of the circulatory system. Experimentally, it is impossible to include all known variables in a single system. However, by modeling the new HEMS model segmentally instead of monolithic approach; it also gives the opportunity to evaluate a group of variables at the same time and even to examine the interaction between the variables.

The partial description of dynamic models in the new HEMS is usually made with a set of differential equations using

hydraulic parameters. Different behaviours are observed in various parts of the closed loop. As a result, it is possible to evaluate a group of variables at the same time and even to examine the interaction between variables. The new version of the hydro-electro-mechanical system of human heart is modelled through integrated 14 series circuits of electrical equivalent of sub-segments of heart, the integrated form of all subsystems making up the total heart and its total functionality.

The total and integrated equivalent circuit of this new HEMS model, a fully equivalent closed-circuit, was developed from the cardiovascular system structure given in Fig. 4 and physiological values used for this model are given in Table II. The pressure and flow values of the time-dependent outlets, using the values in Table II, are given by the following equations; derived for different segments of our model, respectively.

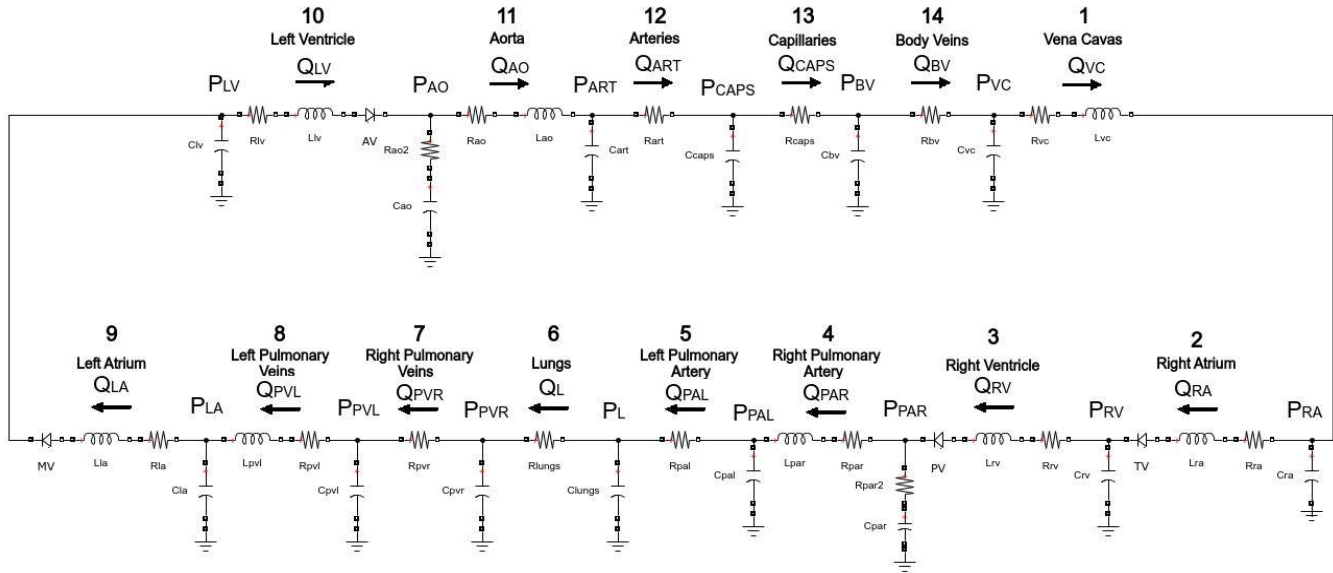


Fig. 4. Integrated Equivalent Circuit of the HEMS

In equations (8) and (9), time-dependent average pressure (P_{VC}) and flow (Q_{VC}) equations are obtained for the superior and inferior vena cava sections of the heart:

$$P_{VC}(t) = \frac{V_{VCI}(t) - V_{VCU}(t)}{C_{vc}} \quad (8)$$

$$\frac{dQ_{VC}(t)}{dt} = \frac{P_{VC}(t) - P_{RA}(t) - [R_{vc} \cdot Q_{VCI}(t)]}{L_{vc}} \quad (9)$$

In equations (10) and (11), time-dependent average pressure (P_{RA}) and end-diastolic flow (Q_{RAD}) equations are obtained for the right atrium of the heart:

$$P_{RA}(t) = \frac{V_{RAI}(t) - V_{RAU}(t)}{C_{ra}} \quad (10)$$

$$\frac{dQ_{RAD}(t)}{dt} = \frac{P_{RA}(t) - P_{RV}(t) - [R_{ra} \cdot Q_{RAI}(t)]}{L_{ra}} \quad (11)$$

In equations (12) and (13), time-dependent average pressure (P_{RV}) and end-diastolic flow (Q_{RVD}) equations are obtained for the right ventricular segment of the heart, where C_{rv} is the compliance of the right ventricle.

$$P_{RV}(t) = \frac{V_{RVI}(t) - V_{RVU}(t)}{C_{rv}} \quad (12)$$

$$\frac{dQ_{RVD}(t)}{dt} = \frac{P_{RV}(t) - P_{PAR}(t) - [R_{rv} \cdot Q_{RVI}(t)]}{L_{rv}} \quad (13)$$

In equations (14) and (15), time-dependent average pressure (P_{PAR}) and flow (Q_{PAR}) equations are obtained for the right pulmonary arteries:

$$P_{PAR}(t) = \frac{V_{PARI}(t) - V_{PARU}(t)}{C_{par}} + R_{par2} \cdot [Q_{RVI}(t) - Q_{PARI}(t)] \quad (14)$$

$$\frac{dQ_{PAR}(t)}{dt} = \frac{P_{PAR}(t) - P_{PAL}(t) - [R_{par} \cdot Q_{PARI}(t)]}{L_{par}} \quad (15)$$

In equations (16) and (17), time-dependent average pressure (P_{PAL}) and flow (Q_{PAL}) equations are obtained for the left pulmonary arteries:

$$P_{PAL}(t) = \frac{V_{PALI}(t) - V_{PALU}(t)}{C_{pal}} \quad (16)$$

$$Q_{PAL}(t) = \frac{P_{PAL}(t) - P_L(t)}{R_{pal}} \quad (17)$$

In equations (18) and (19), time-dependent average pressure (P_L) and flow (Q_L) equations are obtained for the lungs segment of the heart:

$$P_L(t) = \frac{V_{LI}(t) - V_{LU}(t)}{C_{lungs}} \quad (18)$$

$$Q_L(t) = \frac{P_L(t) - P_{PVR}(t)}{R_{lungs}} \quad (19)$$

In equations (20) and (21), time-dependent average pressure (P_{PVR}) and flow (Q_{PVR}) equations are obtained for the right pulmonary veins:

$$P_{PVR}(t) = \frac{V_{PVRl}(t) - V_{PVRu}(t)}{C_{pvr}} \quad (20)$$

$$Q_{PVR}(t) = \frac{P_{PVR}(t) - P_{PVL}(t)}{R_{pvr}} \quad (21)$$

In equations (22) and (23), time-dependent average pressure (P_{PVL}) and flow (Q_{PVL}) equations are obtained for the left pulmonary veins:

$$P_{PVL}(t) = \frac{V_{PVLl}(t) - V_{PVLu}(t)}{C_{pvl}} \quad (22)$$

$$Q_{PVL}(t) = \frac{P_{PVL}(t) - P_{LA}(t)}{R_{pvl}} \quad (23)$$

In equations (24) and (25), time-dependent average pressure (P_{LA}) and end-diastolic flow (Q_{LAD}) equations are obtained for the left atrium of the heart:

$$P_{LA}(t) = \frac{V_{LAl}(t) - V_{LAU}(t)}{C_{la}} \quad (24)$$

$$\frac{dQ_{LAD}(t)}{dt} = \frac{P_{LA}(t) - P_{LV}(t) - [R_{la} \cdot Q_{LAl}(t)]}{L_{la}} \quad (25)$$

In equations (26) and (27), time-dependent average pressure (P_{LV}) and end-diastolic flow (Q_{LVD}) equations are obtained for the left ventricular segment of the heart, where C_{lv} is the compliance of the left ventricle.

$$P_{LV}(t) = \frac{V_{LVl}(t) - V_{LVU}(t)}{C_{lv}} \quad (26)$$

$$\frac{dQ_{LVD}(t)}{dt} = \frac{P_{LV}(t) - P_{AO}(t) - [R_{lv} \cdot Q_{LVl}(t)]}{L_{lv}} \quad (27)$$

In equations (28) and (29), time-dependent average pressure (P_{CAPS}) and flow (Q_{CAPS}) equations are obtained for the capillaries:

$$P_{CAPS}(t) = \frac{V_{CAPSl}(t) - V_{CAPSu}(t)}{C_{caps}} \quad (28)$$

$$Q_{CAPS}(t) = \frac{P_{CAPS}(t) - P_{BV}(t)}{R_{caps}} \quad (29)$$

In equations (30) and (31), time-dependent average pressure (P_{BV}) and flow (Q_{BV}) equations are obtained for the body veins:

$$P_{BV}(t) = \frac{V_{BVl}(t) - V_{BVu}(t)}{C_{bv}} \quad (30)$$

$$Q_{BV}(t) = \frac{P_{BV}(t) - P_{VC}(t)}{R_{bv}} \quad (31)$$

TABLE II. PARAMETERS OF THE HEMS

	R [mmHg.s/ml]	L [mmHg.s ² /ml]	C [ml/mmHg]	P [mmHg]	Initial V _i [ml]	Unstressed V _u [ml]	Initial Q _i [ml/s]
Vena Cavas	14	1	0.0453	7.1	2375.8	1947	85
Right Atrium	4	2	0.0451	5.54	442.23	1949	0
Right Ventricle	6	1	Variable	7.5	154.93	11.1	5.3
Right Pulmonary Artery	11	1	0.00015	7.1	9.29	7.87	0
Right Pulmonary Artery 2	12	-	-	-	-	-	-
Left Pulmonary Artery	41	-	0.00032	6.98	26.36	23.42	-
Lungs	79	-	0.00273	6.5	234.16	210.5	-
Right Pulmonary Veins	31	-	0.0012	4.35	74.96	68	-
Left Pulmonary Veins	9	1	0.0011	3.52	75.16	70	31
Left Atrium	5	1	0.01117	4.35	866.97	814.4	0
Left Ventricle	5	2	Variable	3.9	136.91	10.1	0
Aorta	10	3	0.00017	63.3	49.49	35.15	4.3
Aorta 2	10	-	-	-	-	-	-
Arteries	163	-	0.00024	63	105.16	85	-
Capillaries	1002	-	0.001825	62	861.85	711	-
Body Veins	91	-	0.0212	12.5	1261.3	908	-

III. SIMULATION RESULTS

Pressure waveforms are signals that suggest significant anomalies in the human circulatory system and are used in the diagnosis of cardiovascular diseases, such as heart valve diseases and aneurysms. The left ventricle and aortic pressure-time graph, which is in conformance with the physiological waveform of the circulatory system, shows the time-dependent change of aortic pressure and left ventricular pressure, and as a result of our Matlab based model simulation given in Fig. 5a. This change in pressure difference is related to the resistance parameter of the aortic valve. This structural change was detected by our model simulation. In addition, the comparison of the reference parameters with the theoretical simulation of HEMS model is given in Table III.

The fill in pressures of the ventricles are important in the evaluation of mechanical functions. The fill in pressures of the ventricles due to the blood volume are generally related to the end-diastolic volume (EDV). However, it is also linked to the systolic and diastolic function of the heart. The volume values of left (V_{LV}) and right (V_{RV}) ventricles were calculated based on Matlab based simulation and their time depended graphical changes are given in Fig. 5b. As it can be seen, the stroke volume pumped out of each ventricle is about 60 ml/beat and corresponds to a cardiac output (CO) of 72 ml/s (4.32 l/min) at a heartbeat of 0.83 s. Fill in and stroke volumes are not equal for both ventricles. It is possible that one ventricle passes a little more blood than the other for a heartbeat. However, on average, the fill in and stroke volume must be equal for the left ventricle (LV) and the right ventricle (RV). Although these values were found to deviate slightly from the statistical measurements, the final systolic volume (ESV) and the final diastolic volume (EDV) on average were 150 ml. This means that the value of the ejection fraction $[(EDV - ESV) / EDV]$ is about 50%. This value means that the heart does not function by one half as much as it needs; but it discharges only 50% of the blood into the veins every time it contracts. Ejection fraction (E_F) is a parameter related to stroke volume (SV). Normally, the heart throws more than half of the blood in the ventricles into the veins each time it contracts. E_F shows how much blood is pumping back to the heart with each heartbeat [13].

For our model, Matlab based plots of the change occurring in the pressure and volume in the left ventricle during a cardiac cycle is shown in Fig. 5c. To assess ventricular performance, a pressure-volume cycle parallel to the normal cardiac cycle was developed. According to this cycle, left ventricular contraction begins at the end of the diastole. The contraction energy is first used to increase the intra-cavity pressure without changing the left intra-ventricular volume. At this stage, the aortic and mitral valves close. The pressure increase continues until the diastolic pressure of the aorta is reached. At this point, the aortic valves open. Myocardial fibers continue to shorten at this stage and intra-ventricular blood is thrown towards the aorta. At this point, intra-ventricular pressure remains constant, but the volume gradually decreases due to ejection. At the end of systole, left ventricular contraction reaches its peak, relaxation begins in myocardial fibers, and when intra-ventricular pressure falls below aortic diastolic pressure, aortic valves close, ejection ends. After that, ventricular relaxation gains speed and

intra-ventricular pressure decreases rapidly without any change in volume. When the ventricular pressure falls below the pressure of the left atrium, the mitral valve opens and the diastolic filling begins. At this stage, the left ventricular volume begins to increase, but a slight increase in pressure occurs, and at the end of this stage, the left ventricular pressure-volume ring is completed.

In Fig. 5c, 4 points A to D are related to ventricular beat generation. Mitral valve closure and isovolumic contraction at point (A), aortic valve opening and ejection phase at point (B), aortic valve closure and isovolumic relaxation at point (C) and ventricular filling occur with mitral valve opening at point (D). The end-diastolic volume (EDV) below indicates the inactive ventricle, and the end-systolic volume relationship (ESV) indicates the active phase of the ventricle.

The amount of blood to be pumped in a continuous cycle determines the amount of blood in the cycle entering the heart from the vena cava. Due to the increase in the amount of online blood entering the ventricles, the ventricles go under high stress due to the specialized muscular structure of the heart, and they contract strongly and increase the amount of blood pumped by the heart. This cycle follows the Frank-Starling Law, which states that only the amount of quantity of blood entering the heart can only be pumped out into the cycle. In this way, the heart can pump only the amount of blood it already possess [14].

The basic mechanism underlying the Frank-Starling law is proportional to the contractility levels in the heart muscle fibers. The factor that increases the end-diastolic volume (EDV) is caused by the increase in venous return to the heart; this increase expands the ventricles in volume, stretches the heart muscle fibers, increases stroke volume and consequently cardiac output (CO). In addition, the increase in sympathetic stimulation increases the contraction force of the ventricle, so the ventricles pump more blood in systole and the end systolic volume (ESV) decreases. In cases where sympathetic stimulation increases, for example due to the effects of exercise, the contraction force of the ventricles increases and more blood is pumped, consequently the amount of blood remaining in the ventricles decreases. In line with this basic physiological condition, Matlab based system simulations showing the temporal variation of left ($SLV=1/C_{LV}$) and right ($SRV=1/C_{RV}$) ventricular stiffness from heart components were created and the results are given in Fig. 5d.

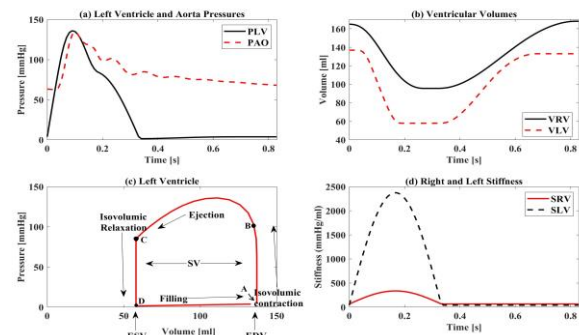


Fig. 5. (a) Simulated left ventricular pressure (P_{LV} -mmHg) and aortic pressure (P_{AO} -mmHg). (b) Simulated right ventricle volume (V_{RV} -ml) and left ventricle volume (V_{LV} -ml). (c) Simulated of pressure-volume change in the left ventricle. (d) S_{LV} : Left Ventricular Stiffness (mmHg / ml) and S_{RV} : Right Ventricular Stiffness (mmHg / ml).

TABLE III. COMPARISON BETWEEN NORMAL VALUES [15] AND THE NEW HEMS VALUES IN SOME PARTS OF THE HEART

Hemodynamic Parameters		
Parameter	Normal Range	HEMS Range
Cardiac Output (CO)	4-8 l/min	4.32 l/min
Stroke Volume (SV)	60-100 ml/beat	60 ml/beat
Ejection Fraction (EF)	40-60%	50%
Right Ventricular Volume (V_{RV})	100-160 ml	100-154.93 ml
Left Ventricular Volume (V_{LV})	60-140 ml	60-136.91 ml
Arterial Blood End-Diastolic Pressure (P_{ARTD})	60-90 mmHg	63 mmHg
Right Atrial End-Diastolic Pressure (P_{RAD})	2-6 mmHg	5.54 mmHg
Right Ventricular End-Diastolic Pressure (P_{RVD})	2-8 mmHg	7.5 mmHg
Left Atrial End-Diastolic Pressure (P_{LAD})	4-12 mmHg	4.35 mmHg

IV. CONCLUSIONS

In this paper, the main focus of the new HEMS modelling is to define the dynamic properties of the cardiovascular system with mathematical equations and the system behaviour based on a strong theoretical background. The dynamic properties of the cardiovascular system are determined by a set of ordinary differential equations. The system was solved using an ordinary differential equation method, known as Ode23, proper enough to be used in the solution of a closed-loop cardiovascular system until it converges. In addition, the whole circuit of the heart cycle acts as a time vector, with initial values taken from the system, it was simulated for 0.83 second with Matlab based Ode23 method and were obtained time-dependent curves of the outputs of pressure, volume and flow, accordingly. If computation time has priority and a high level of accuracy is desired, then Ode23 is the best alternative for such applications. For our model, the Ode23 is more efficient choice than the other types of ODEs [16].

In addition, Matlab Ode23, which is preferred for our model, is within the scope of a performance improvement with other odes (TABLE IV). According to this comparison, Ode23 compared to other odes; successful steps and failed attempts in the calculation seem to be superior.

Ode solvers, estimate the local error in different components of the solution at each step. This error is considered as a function of the specified relative tolerance (RelTol) and the specified absolute tolerance (AbsTol). Accuracy values were created according to different error values in our model, and convergence values were calculated according to these error values in Table IV. According to this table, as the relative tolerance (RelTol) and absolute tolerance (AbsTol) values are both decreased, then the calculation time decreases and the performance of Ode23 increases with respect to the performance of other odes.

TABLE IV. COMPARISON OF ODE23, ODE45 AND ODE113 FOR THE NEW HEMS.

Solver	Elapsed Time (s)	Successful Steps	Failed Attempts	Function Evaluation
RelTol: 1e-3 - AbsTol: 1e-6				
Ode23	0.581493	2970	707	8266
Ode45	0.726103	914	1080	9727
Ode113	1.356708	1675	1551	7492
RelTol: 1e-12 - AbsTol: 1e-14				
Ode23	0.398419	2970	707	8266
Ode45	0.398793	914	1080	9727
Ode113	0.882071	1675	1551	7492

The new developed version of cardiovascular system (HEMS model) given in this paper is a new version of the HEMS model, using many variables and their interactions accordingly. Autocad based anatomical 3D drawings of all subsystems in the heart system were drawn targeting specific modelling and physiological-anatomical requirements. This is applied to facilitate intermediate version development to achieve the more integrated HEMS model possible, such as its multi-layer equivalents using electrical, mechanical and hydraulics parameters all together in an integrated model. Because, in order to integrate nonlinear complex biological structures and independent modelling, structures that can be described as interface models are needed. Biological and anatomical structures that act as multi-functional intelligent elements or systems can only be examined in a single form only as an electrical, mechanical or hydraulic system, by ignoring their multi-functionalities and based on their functions reduced to a single dominant function.

Our model defines the start time of the cardiac cycle as the time instant at which contraction of the right atrial wall becomes active due to action potentials. In order to represent the contraction and relaxation changes in each cardiac chamber, a time-dependent activation function was created for the ventricle and atria. Right and left ventricles are modelled as time-varying capacitors due to their flexible characteristics and activation function. The flow waveform was simulated to describe the systole and diastole phases of the cardiac cycle. The new HEMS model can integrate the cardiac dynamics and evaluate a group of variables, at the same time creating an efficient platform to study combinations of physiological properties as well as the effects of modifications in the system dynamics. The new version of the hydro-electro-mechanical system is modelled through 14 series of electrical circuits in which the integrated forms of all subsystems that make up the whole heart are produced by creating unique equivalent electrical circuits. By comparing our model with available hemodynamic models [17, 18], our proposed model is a more comprehensive model than other minimal models that can be used to evaluate the real time implementations.

Time-dependent average pressure measurement is a key tool to diagnose various heart diseases, which is one of the main reasons that this paper focused on the mathematical description of the average pressure of each segment of the whole the cardiovascular system (CVS) resulting in 28 equations (Eq. 4 –

Eq. 31). Additionally, Fig.5 gives the time-dependency of the critical four outputs which are graphically represented.

The graphics and values obtained are in conformance with the physiological values of the healthy subject and literature data available. As a result, it is predicted that the physiological system parameters based new HEMS model will act as a new method in the diagnosis of diseases and cardiovascular disorders involving the human heart through pressure-volume relationships and hemodynamic parameters.

V. FUTURE WORK

Engineering equivalent new models of the cardiovascular system are expected to make deeper understanding of complex processes possible occurring in the heart and blood vessels under the normal and pathophysiological conditions. All outputs obtained from or derived from pressure-volume relations or evaluated hemodynamic variables may serve as a useful assistant tool for diagnosing an illness and then recommending the new way of medical treatment of the cardiovascular disorders. The new HEMS model is thought to be potentially beneficial for hemodynamic simulation of diseases, cardiovascular disorders as well as congenital heart diseases, for example ASD, VSD and PDA, involving the human heart and its real-time simulation. The new HEMS model will be further developed and enhanced to improve the understanding of complex hemodynamic states and validation through patient data.

Abbreviations

The following abbreviations are used in this article:

HEMS	Hydro-electro-mechanical system
WM	Windkessel Model
CVS	Cardiovascular System
SA	Sinus Node or Sinoatrial Node
HP	Heart Period
AF	Activation Function
EDV	End-Diastolic Volume
ESV	End-Systolic Volume
E_F	Ejection Fraction
CO	Cardiac Output
SV	Stroke Volume
SLV	Left Ventricular Stiffness
SRV	Right Ventricular Stiffness
ASD	Atrial Septal Defect
VSD	Ventricular Septal Defect
PDA	Patent Ductus Arteriosus

REFERENCES

- [1] O. Frank, "Die Grundform des arteriellen Pulses. Erste Abhandlung. Mathematische Analyse." *Z. Biol.* 37, 483–526, 1899. DOI: 10.1016/0022-2828(90)91459-k.
- [2] Rosalia L., Ozturk C., Van Story D., Horvath M.A. and Roche E.T., "Object-Oriented Lumped-Parameter Modeling of the Cardiovascular System for Physiological and Pathophysiological Conditions.", *Adv. Theory Simul.*, 4: 2000216, 2021. DOI:10.1002/adts.202000216.
- [3] Westerhof B.E., Van Gemert M.J.C. and Van den Wijngaard J.P., "Pressure and Flow Relations in the Systemic Arterial Tree Throughout Development From Newborn to Adult.", *Front. Pediatr.* 8:251, 2020. DOI: 10.3389/fped.2020.00251.
- [4] Ajmal A., Tananant B., Andres J. R., Vinh N. D. L., Jessica C. R., "Investigation of optical heart rate sensors in wearables and the influence of skin tone and obesity on photoplethysmography (PPG) signal," *Proc. SPIE 11638, Biophotonics in Exercise Science, Sports Medicine, Health Monitoring Technologies, and Wearables II*, 1163808, 2021. DOI:10.1117/12.2578023.
- [5] Padmos R.M., Józsa T.I., El Bouri W.K., Konduri P.R., Payne S.J., Hoekstra A.G., "Coupling one-dimensional arterial blood flow to three-dimensional tissue perfusion models for in silico trials of acute ischaemic stroke.", *Interface Focus* 11:20190125, 2021. DOI:10.1098/rsfs.2019.0125.
- [6] Morany, A., Lavon, K., Bluestein, D. et al., "Structural Responses of Integrated Parametric Aortic Valve in an Electro-Mechanical Full Heart Model.", *Ann Biomed Eng* 49, pp. 441–454, 2021. DOI: 10.1007/s10439-020-02575-0.
- [7] Roy D., Mazumder O., Sinha A. and Khandelwal S., "Multimodal cardiovascular model for hemodynamic analysis: Simulation study on mitral valve disorders." *Plos One*, Vol. 16(3):e0247921, 2021. DOI:10.1371/journal.pone.0247921.
- [8] S. Shimizu, D. Une and T. Kawada, "Lumped parameter model for hemodynamic simulation of congenital heart diseases", *The Journal of Physiological Sciences*, Vol. 68, pp. 103–111, 2018. DOI: 10.1007/s12576-017-0585-1.
- [9] F. Yalcinkaya, E. Kizilkaplan and A. Erbas, "Mathematical modelling of human heart as a hydroelectromechanical system", *8th International Conference on Electrical and Electronics Engineering (ELECO)*, Bursa, 2013. DOI:10.1109/ELECO.2013.6713862.
- [10] Trzaska Z., "Study of mixed-mode oscillations in a nonlinear cardiovascular system." *Nonlinear Dyn* 100, 2635–2656, 2020. DOI: 10.1007/s11071-020-05612-8.
- [11] Jamie R. M., and Jiun W., "Expanding application of the Wiggers diagram to teach cardiovascular physiology.", *The American Physiological Society*, Vol. 38:2, pp. 170-175, 2014. DOI: 10.1152/advan.00123.2013.
- [12] V. S. Vasudevan, K. Rajagopal, J. F. Antaki, "Application of mathematical modeling to quantify ventricular contribution following durable left ventricular assist device support", *Applications in Engineering Science* 2022, Vol. 11, ISSN 2666-4968. DOI: 10.1016/j.apples.2022.100107.
- [13] Otto A. Smiseth, John M Aalen, Helge Skulstad, "Heart failure and systolic function: time to leave diagnostics based on ejection fraction?", *European Heart Journal*, Vol. 42:7, 14 February 2021, pp. 786–788, 2021. DOI: 10.1093/eurheartj/ehaa979.
- [14] June-Chiew H., Denis L., Andrew T. and Kenneth T., "Re-visiting the Frank-Starling nexus", *Progress in Biophysics and Molecular Biology*, Vol. 159, pp. 10-21, 2021. DOI:10.1016/j.pbiomolbio.2020.04.003.
- [15] Cattermole G.N., Leung P.Y., Ho G.Y., et al., "The normal ranges of cardiovascular parameters measured using the ultrasonic cardiac output monitor." *Physiol Rep.* 2017; 5(6):e13195. DOI:10.14814/phy2.13195.
- [16] Comunale G., Peruzzo P., Castaldi B. et al., "Understanding and recognition of the right ventricular function and dysfunction via a numerical study", *Sci Rep* 11, 3709, 2021. DOI:10.1038/s41598-021-82567-9.
- [17] Bahnasawy S., Al-Sallami H., Duffull S., "A minimal model to describe short-term haemodynamic changes of the cardiovascular system." *Br J Clin Pharmacol* 2021; 87: 1411–1421. DOI:10.1111/bcp.14541.
- [18] Roy D., Mazumder O., Sinha A. and Khandelwal S., "Multimodal cardiovascular model for hemodynamic analysis: Simulation study on mitral valve disorders." *PLoS ONE* 2021; 16(3):e0247921. DOI:10.1371/journal.pone.0247921.

BIOGRAPHIES



Fikret YALCINKAYA received his B.Sc. degree in Electrical and Electronics Engineering from METU, Turkey (1984). He received his integrated Ph.D. degrees in Biomedical Engineering from Engineering and Applied Sciences department of the University of Sussex, UK (1994-

1998).

Since 2001, he has been an Assistant Professor with Electrical and Electronics Engineering Department, Kirikkale University, Kirikkale, Turkey.

His research interests include nanobiosensors, medical instrumentation, physiological modelling (cardiovascular system, respiratory system and auditory system) and medical imaging (specifically CNN and Deep Learning based melanoma early detection).



Ertem KIZILKAPLAN received his B.Sc. degree in Electrical and Electronics Engineering from Kirikkale University, Kirikkale, Turkey (2010) and M.Sc degree in Electrical and Electronics Engineering from Kirikkale University, Kirikkale, Turkey (2022). Since 2010, he has been working as an Electrical and Electronic

Engineer at MSK Immobilien Invest GmbH.

His research interests include mathematical modelling, physiological modelling (cardiovascular system), heart diseases and biomedical research.